Observation of bulk band dispersions of YbRh$_2$Si$_2$ using soft x-ray angle-resolved photoemission spectroscopy

A. Yasui,[1,*] Y. Saitoh,[1] S.-i. Fujimori,[1] I. Kawasaki,[1] T. Okane,[1] Y. Takeda,[1] G. Lapertot,[2] G. Knebel,[2] T. D. Matsuda,[3] Y. Haga,[3] and H. Yamagami[1,4]

[1]*Condensed Matter Science Division, Japan Atomic Energy Agency, Sayo, Hyogo 679-5148, Japan*
[2]*DRFMC, SPSMS, CEA Grenoble, 17 rue des Martyrs, 3805-4 Grenoble Cedex 9, France*
[3]*Advanced Science Research Center, Japan Atomic Energy Agency, Tokai, Ibaraki 319-1195, Japan*
[4]*Department of Physics, Kyoto Sangyo University, Kyoto 603-8555, Japan*

We have performed soft x-ray angle-resolved photoemission spectroscopy (ARPES) measurements on YbRh$_2$Si$_2$ and clarified its three-dimensional bulk valence-band structures. The ARPES spectra have not only Yb^{3+} multiplet peaks but also a finite contribution of Yb^{2+} peaks at 15 K, corresponding to the valence fluctuating behavior in this compound. This means that Yb $4f$ electrons in this compound have itinerant character below the T_K. We have found that dispersions of the valence bands except the vicinity of the Yb $4f$ bands agree better with those of the band-structure calculation of LuRh$_2$Si$_2$ than those of YbRh$_2$Si$_2$ within a local-density approximation. In addition, the Yb $3d$-$4f$ resonant photoemission spectra of YbRh$_2$Si$_2$ strongly suggest the existence of Yb $5d$ electrons in the valence band. We conclude that the charge transfer from the Yb $4f$ state to the Yb $5d$ state has an important role in the formation of the valence band of YbRh$_2$Si$_2$.

　　　　　　　PACS number(s): 71.27.+a, 71.20.Eh, 79.60.−i

I. INTRODUCTION

The heavy fermion states which are characterized by the huge effective mass of electrons are deeply related with attractive physical properties such as quantum critical phenomena or superconductivities in strongly correlated f-electron materials. A heavy fermion compound YbRh$_2$Si$_2$ has an extremely large electronic specific-heat coefficient of $\gamma = 1.7$ J/(mol K^2)[1] and shows antiferromagnetic ordering in the ground state with the Neel temperature of $T_N = 70$ mK.[2] This extremely heavy electron mass and very small T_N suggest that YbRh$_2$Si$_2$ locates near a quantum critical point (QCP). In fact, YbRh$_2$Si$_2$ can be tuned through the QCP by the small change of various control parameters such as the application of the magnetic field[1] or the substitution of Ge for Si.[3] By increasing the applied magnetic field, the Hall coefficient becomes suddenly large when it reaches the critical value of $H_c \sim 0.06$ T for $H \perp c$.[4] Thus, above H_c, it is thought that Yb $4f$ electrons, which are completely localized at the Yb site below H_c, are related to the formation of Fermi surfaces (FSs) and the FS size suddenly becomes large. The various mechanisms for this behavior have been proposed, such as a breakdown of the Kondo effect (Kondo breakdown),[5] a Lifshitz transition driven by the Zeeman splitting,[6] or a critical Yb valence fluctuation.[7]

Many electronic structure studies, such as quantum oscillation measurement and angle-resolved photoemission spectroscopy (ARPES), have been performed to understand the nature of the QCP of YbRh$_2$Si$_2$. Quantum oscillation measurements claimed that the shape of the FSs resembles the "small FS" where Yb $4f$ electrons do not participate and which is obtained by the band calculation within a local-density-approximation (LDA) of LuRh$_2$Si$_2$, rather than the "large FS" where Yb $4f$ electrons do participate and which is obtained by that of YbRh$_2$Si$_2$.[8] However, they also concluded that both of the theoretical pictures are insufficient to explain the experimental results. For example, both the pictures cannot

explain the angle dependence of the "J" branch originated from the jungle-gym-like shape of the FS. Therefore, the electronic structure has not been well understood yet, and appropriate theoretical treatments of its electronic structure are still an open question. In order to understand the nature of the QCP as well as to provide a guideline for more advanced band-structure calculations, it is important to determine not only the FSs but also the band structures below the Fermi level experimentally.

ARPES is a powerful experimental tool to study the electronic structure of materials because it can observe valence-band structures and FSs directly. Recently, we have carried out the soft x-ray (SX) ARPES measurements for YbCu$_2$Ge$_2$.[9] YbCu$_2$Ge$_2$ has the ThCr$_2$Si$_2$-type crystal structure the same as YbRh$_2$Si$_2$, and it had been thought that YbCu$_2$Ge$_2$ is a Yb divalent compound. In contrast, our SX-ARPES study of YbCu$_2$Ge$_2$ clarified that Yb $4f$ electrons contribute to the formation of FSs through hybridization with conduction electrons, something which was not found by the other experiments including quantum oscillation measurements. Additionally, we have observed its three-dimensional (3D) band structures in this measurement and found that those of YbCu$_2$Ge$_2$ can be explained reasonably by a relativistic LDA calculation.

ARPES studies on YbRh$_2$Si$_2$ have been intensively performed. However, these studies were performed by using low-energy incident photons of $h\nu < 120$ eV.[10] One of the advantages of the low-energy ARPES experiments is a very high-energy resolution. Vyalikh *et al.* have observed the crystal electric field splitting of Yb $4f$ bands in an energy order of 10 meV just below the Fermi level and its hybridization with valence bands by using the vacuum ultraviolet (VUV) radiation.[11] However, for the Yb-based compounds, the VUV ARPES spectra are generally dominated by contributions from surface-originated Yb $4f$ states. Especially, the shape of valence bands in the bulk state is influenced by the hybridization with the surface Yb^{2+} $4f$ bands.[10] This makes

it difficult to determine the bulk valence-band dispersions. Furthermore, it is difficult to obtain 3D band structures by using the VUV ARPES experiments due to their lower k_z resolution originating from the short escape depth of photoelectrons. Very recently, Mo *et al.* have studied the temperature dependence of the quasiparticle peaks just below the Fermi energy E_F, using a 7-eV laser photon source.[12] The laser ARPES, however, has limitations on the accessible ranges on the momentum and the energy due to its low photon energies. Thus, the low-energy ARPES experiments are not suitable for the investigation of overall bulk valence-band structures.

In the present study, we have performed SX-ARPES measurements to investigate 3D valence-band dispersions in the bulk state of YbRh$_2$Si$_2$. It is expected that a use of incident photons in the SX region suppresses the surface contributions. By comparing band dispersions of the experiment and the LDA calculation results, we have tested the validity of the "large FS" picture and the "small FS" picture. In addition, we discuss the influence of interactions between Yb 4f electrons and conduction bands on the valence-band structures.

II. EXPERIMENT AND CALCULATION

SX-ARPES measurements were recorded at the photoemission endstation equipped with a VG-SCIENTA SES2002 electron analyzer at the twin-helical undulator beamline BL23SU of SPring-8. The energy resolution was set to be about 130 meV at $h\nu = 860$ eV. In order to obtain the clean surface, the samples were cleaved under ultrahigh vacuum conditions with a base pressure of 1.0×10^{-8} Pa. The inner potential was estimated to be 12 eV from the incident photon energy dependence of the ARPES spectra. The ARPES spectra were taken in the paramagnetic state at 15 K, well below the Kondo temperature T_K of $\sim$25 K.[2] We confirmed that O 1s peaks were not observed before and after the SX-ARPES measurements.

LDA band calculations have been carried out for YbRh$_2$Si$_2$ and LuRh$_2$Si$_2$ with the relativistic linearized augmented plane-wave (RLAPW) method.[13] This calculation incorporates the spin-orbit (SO) interaction into the Hamiltonian without a second variational approximation. We utilized the lattice parameters of $a = 4.007$ Å, $c = 9.858$ Å, and $z_{Si} = 0.3791$ in both calculations.[14] During the self-consistent calculation of YbRh$_2$Si$_2$, the electrons of the $4f^{14}$ and $6s^2$ configurations at the Yb site, $4d^8$ and $5s^1$ at the Rh site, and $3p^2$ and $3s^2$ at the Si site are calculated as valence electrons, while the other electrons are treated as core electrons. For LuRh$_2$Si$_2$, one 5d electron is added to the valence electrons in the electronic configuration of YbRh$_2$Si$_2$.

III. RESULTS AND DISCUSSION

A. SX-ARPES spectra

In Fig. 1(a), we show an intensity map of SX-ARPES spectra measured along several high-symmetry lines denoted by red lines in the Brillouin zone of this compound shown in Fig. 1(b). The ARPES spectra along the Z-Γ line are obtained by scanning incident photon energies $h\nu = 750$–900 eV, corresponding to the blue stripe plane. Meanwhile, those of

the Γ-X-Z-Γ lines are obtained by changing photoelectron detection angles and fixing the incident photon energy to $h\nu = 860$ eV, corresponding to the orange plane. Each spectrum is normalized with the integrated intensity of its energy-distribution curve (EDC). An angle-integrated PES (AIPES) spectrum obtained at $h\nu = 860$ eV is exhibited in the right side of the ARPES spectra. In the SX region, the contributions from the Yb 4f and the Rh 4d states are much larger than those of the other states. The ratio of the photoionization cross sections is Yb 4f: Rh 4d: other $\sim$1 : 1/10 : 1/100 at $h\nu = 860$ eV according to an atomic calculation.[15] Thus, those spectra are mainly dominated by the contribution from the Yb 4f and the Rh 4d states.

Figures 1(c) and 1(d) show energy-band dispersions and density of states (DOS) of YbRh$_2$Si$_2$ and LuRh$_2$Si$_2$ calculated by using the RLAPW method, respectively. Yb 4f and Rh 4d components in each band are colored by red and blue, respectively. The calculated DOSs are made up mainly of Yb (or Lu) 4f and Rh 4d states. Since LuRh$_2$Si$_2$ has one more 5d electron than YbRh$_2$Si$_2$ and the 5d energy level is higher than the 4f one, the energies of Lu 4f bands are pulled down and they are completely filled.

In Fig. 1(a), two flat bands located at the E_F and the binding energy of $E_B = 1.28$ eV are attributed to the Yb^{2+} $4f_{7/2}$ and the Yb^{2+} $4f_{5/2}$ SO split states, respectively. The doublet structure of Yb^{2+} 4f states comes from the transition from the $4f^{14}$ to the $4f^{13}$ state, and it can be described by the one-electron ground state of the RLAPW calculation for YbRh$_2$Si$_2$ [Fig. 1(c)], because the relativistic band calculations based on the Dirac equation incorporate the SO interaction into the Hamiltonian within the LDA framework, as discussed in our previous paper.[9] The observed Yb^{2+} 4f bands are located in lower binding energies than those obtained by the calculation in which $4f_{7/2}$ states are located at 0.23 eV and $4f_{5/2}$ states at 1.57 eV. Nevertheless, the experimental SO split energy E_{SO} is 1.28 eV, which is in good agreement with the calculated one of 1.34 eV. This value is almost identical to that of a nearly Yb divalent compound YbCu$_2$Ge$_2$ ($E_{SO} = $ 1.3 eV).[9] Therefore, the SO split energy seems to be determined mainly by not the electronic state but the atomic potential. The ARPES spectra reflect bulk valence-band structures because the surface Yb^{2+} 4f bands, which should be located in the higher E_B side of bulk Yb^{2+} bands, are hardly observed. It should be noted that weak peak structures at $E_B = 0.9$ and 2.1 eV of the AIPES spectrum are originated from Rh 4d bands as mentioned below.

Strongly dispersive bands observed in $E_B = 0$–6 eV are contributions mainly from Rh 4d states. The shape of them well corresponds to that of both calculated results of YbRh$_2$Si$_2$ and LuRh$_2$Si$_2$ shown in Figs. 1(c) and 1(d), respectively. For example, there are parabolic bands with a maximum at 0.9 eV and a minimum at 5 eV at the Z point in the experiment as well as both the calculations. At $E_B = 0.9$ and 2.1 eV, several band tops and flat bands with large intensity are found in the ARPES spectra, and they are the origin of the weak peak structures in those energies in the AIPES spectrum. A multiple-peak structure observed in $E_B = 6$–13 eV is the Yb^{3+} multiplet structure, which comes from the transition from the $4f^{13}$ to the $4f^{12}$ state. Since both Yb^{2+} and Yb^{3+} states are observed in the PES spectra, YbRh$_2$Si$_2$ is a valence fluctuation
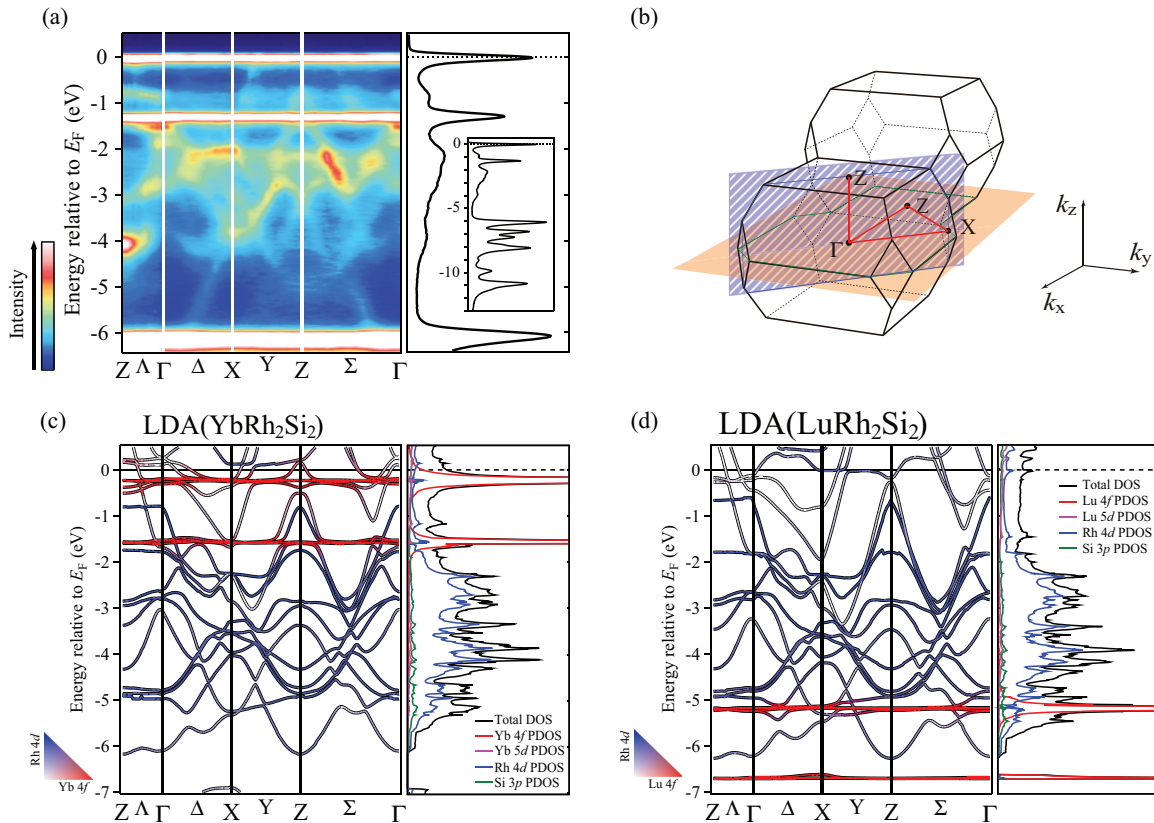
FIG. 1. (Color online) (a) Intensity map of SX-ARPES spectra along several high-symmetry lines denoted by red lines in (b). An angle-integrated PES spectrum obtained at $h\nu = 860$ eV is shown in the right side of the SX-ARPES spectra. (b) Brillouin zone of body-centered tetragonal structure. Orange and blue planes denote the measured region in the angle-scanning measurement and the energy-scanning one, respectively. (c), (d) Energy-band dispersions and density of states obtained by the RLAPW calculation of YbRh$_2$Si$_2$ (c) and LuRh$_2$Si$_2$ (d).

compound. The intensity of the Yb^{3+} multiplet structure is much larger than that of the Yb^{2+} doublet structure, and this is consistent with the Yb valence of about 2.9 determined by the resonant inelastic x-ray scattering (RIXS) measurement.[16] The multiplet structure cannot be reproduced by LDA calculations, but it can be reproduced by atomic calculations including intra-atomic electronic correlations.[17]

Here, we focus on the band dispersions in the first 1.5 eV below E_F. We show SX-ARPES spectra along the Γ-X-Z-Γ lines in this energy region in Fig. 2(a). In Fig. 2(b), band positions determined from EDCs (filled circles) and momentum-distribution curves (MDCs) (open diamonds) of ARPES spectra are exhibited. It should be noted that the band positions were extracted from some equivalent **k** spaces to avoid the influence of the matrix element effect. Figures 2(c) and 2(d) are calculated band dispersions of YbRh$_2$Si$_2$ and LuRh$_2$Si$_2$, respectively. The band indices are counted from the bottom of the valence bands. As shown in Fig. 2(c), the Yb^{2+} $4f_{5/2}$ bands are composed mainly of bands 14–16 and the Yb^{2+} $4f_{7/2}$ bands are composed mainly of bands 19–22 in the calculation of YbRh$_2$Si$_2$. As mentioned above, the experimental Yb^{2+} $4f$ bands are located at the lower binding-energy side than those of the calculation. The bands with large Rh $4d$ components are in qualitative agreements among the ARPES spectra and both the calculated results. For example, the observed parabolic bands A and B are well

explained by the calculated bands 16 and 15 of Fig. 2(c), as well as the calculated bands 20' and 19' of Fig. 2(d), respectively. These bands have anticrossing features at the crossing point with the Yb^{2+} $4f_{5/2}$ bands, indicating that the Yb $4f$ electrons are hybridized with the conduction bands. These structures are also observed in YbCu$_2$Ge$_2$.[9] Band C is located at slightly higher binding energies than band 16 of Fig. 2(c) and band 20' of Fig. 2(d), both of which have small Rh $4d$ components. This makes band D extend to the higher binding-energy side than band 17 of Fig. 2(c) and band 21' of Fig. 2(d).

Both the calculated results have similar band dispersions except for the vicinity of $4f$ bands. Moreover, the band positions in both the calculations deviate from the experimental band positions, and this might be the origin of the difficulties regarding the interpretation of the quantum oscillation results.[8] There is not so much of a difference between the calculated results of YbRh$_2$Si$_2$ and LuRh$_2$Si$_2$ regarding the deviation of the band positions from the experimental one. However, there is a striking difference in the calculated band dispersions between YbRh$_2$Si$_2$ and LuRh$_2$Si$_2$ around the X point, as shown in Figs. 3(c) and 3(d), respectively. It should be mentioned that, in Figs. 3(c) and 3(d), we pick out the Yb $5d$ (pink) and the Rh $4d$ (blue) contributions especially. Bands 17 and 18 of YbRh$_2$Si$_2$ correspond to bands 21' and 22' of LuRh$_2$Si$_2$, respectively. The band shape and the energy position of band 21' are in good agreement with those of band 17. On the other
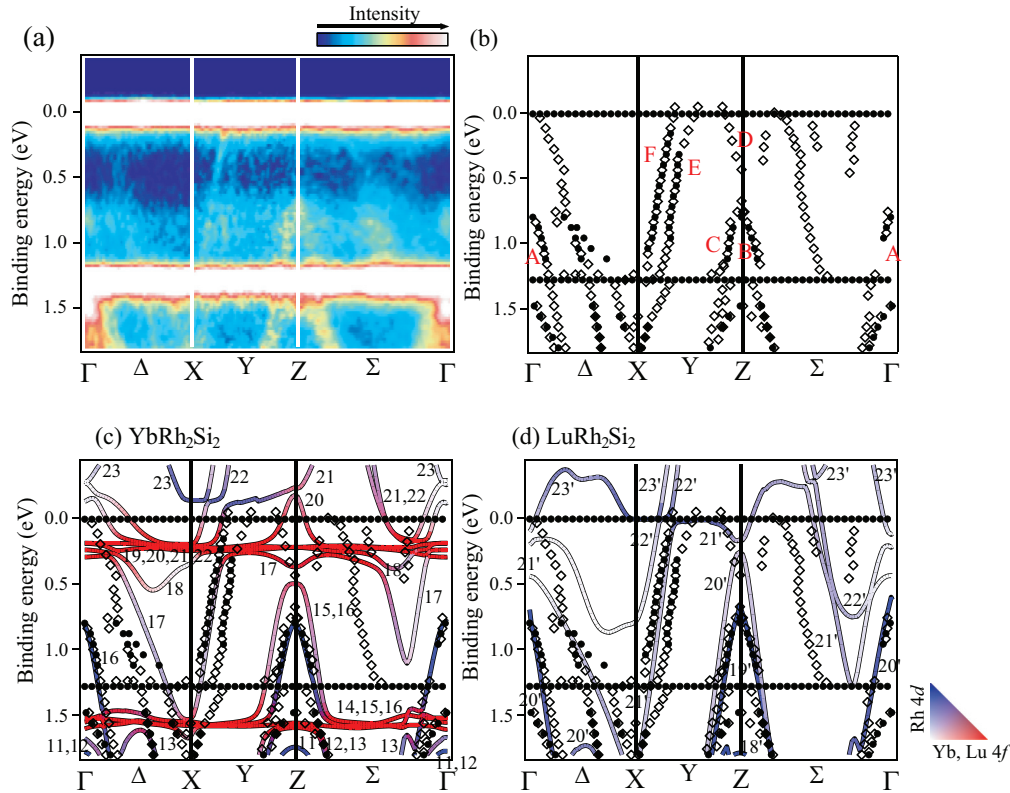
FIG. 2. (Color online) (a) Intensity map of SX-ARPES spectra near E_F region. (b) Band positions determined from EDCs (filled circles) and MDCs (open diamonds). (c), (d) Calculated band dispersions of YbRh$_2$Si$_2$ (c) and LuRh$_2$Si$_2$ (d) together with the experimentally determined band positions. The band indices are counted from the bottom of the valence bands.

hand, band 22' extends to the higher binding-energy side than band 18. Thus, the LDA calculation of LuRh$_2$Si$_2$ has parallel bands of bands 21' and 22' up to E_F around the X point. In the ARPES spectrum, the corresponding bands are bands E and F as shown in Fig. 3(b). Band E has good correspondences to both bands 17 and 21'. On the other hand, band F touches the Yb^{2+} $4f_{5/2}$ bands, and the bands are parallel in ARPES spectra as well as in the calculated result of LuRh$_2$Si$_2$. Therefore, the experimental band dispersions except the Yb $4f$ bands agree better with the LDA calculation for LuRh$_2$Si$_2$. However, this does not mean that the "small FS picture" is applicable to YbRh$_2$Si$_2$, because the experimental bands deviate from the calculated ones of LuRh$_2$Si$_2$ as mentioned above.

We have assumed that the charge transfer from the Yb $4f$ to the Yb $5d$ orbital has an important role in understanding of the electronic structures of YbRh$_2$Si$_2$. We discuss this point using the calculated result of YbRh$_2$Si$_2$ as the starting point. The Yb valence is thought to be determined mainly by the occupation number of Yb $4f$ states. When the Yb valence is 2.9 as obtained by the RIXS measurement,[16] the occupation number of Yb $4f$ states is expected to be 13.1. Meanwhile, the $4f^{14}$ electronic configuration is treated as valence electrons at the Yb site in the YbRh$_2$Si$_2$ calculation, as mentioned above. The 0.9 electrons are moved from the Yb $4f$ orbital to the other state, when the Yb^{2+} $4f_{7/2}$ bands shift to the lower binding-energy side probably due to correlation effects and they cross the Fermi level. Thus, the experimental Yb^{2+} $4f_{7/2}$ bands should be located at lower binding energies than the calculated ones. In addition, because the SO split energy

is mainly determined by the atomic number, the SO split counterpart Yb^{2+} $4f_{5/2}$ bands are also shifted toward the lower binding-energy sides. When the electrons which had belonged in Yb $4f$ states enter into the Yb $5d$ orbital, the electronic states except for the Yb $4f$ states are similar to those of LuRh$_2$Si$_2$. As shown in Fig. 3(c), band 18 originally has relatively large Yb $5d$ components. Therefore, the shape of band F could be explained by the calculation of YbRh$_2$Si$_2$ with moving nearly one electron from the Yb $4f$ orbitals to band 18, which has large contributions from the Yb $5d$ states.

B. Yb $3d$-$4f$ resonant PES spectra

In order to investigate whether the Yb $5d$ electrons exist in the valence band experimentally, we have performed Yb $3d$-$4f$ resonant PES measurements of YbRh$_2$Si$_2$. $3d$-$4f$ resonant PES measurements have often been utilized to extract the $4f$ components. Meanwhile, if $5d$ electrons exist in the valence band, the $5d$ component can be enhanced by the $3d$-$4f$ resonant photoemission process. Actually, in the $3d$-$4f$ resonant PES measurements for La-based compounds, some results have indicated the enhancement of the La $5d$ components.[18]

In the Yb^{3+} state with the $4f^{13}$ electronic configuration, since the $4f$ bands exist in the unoccupied state, the Yb $3d$-$4f$ x-ray absorption occurs and the photoelectron intensity for the Yb^{3+} state is enhanced in the resonant photoemission process. On the other hand, in the Yb^{2+} state ($4f^{14}$), all $4f$ bands are located in the occupied state, so that the resonant enhancement
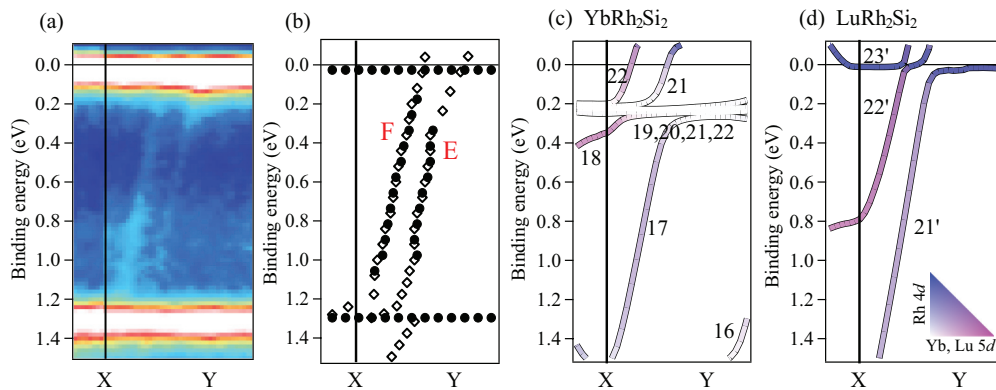
FIG. 3. (Color online) (a), (b) Intensity map of SX-ARPES spectra (a) and band positions (b) at around the X point. (c), (d) Calculated band dispersions of $YbRh_2Si_2$ (c) and $LuRh_2Si_2$ (d). Especially the Yb or Lu 5d (pink) and the Rh 4d (blue) contribution are shown in these plots.

of the Yb^{2+} part cannot be observed. Thus, the resonant enhancement near the Fermi level reveals the existence of the Yb 5d electrons in the valence band, because the energies of the Yb^{3+} state separate from E_F and the Yb 5d states are positioned near E_F in the LDA calculation of $YbRh_2Si_2$.

Figure 4(a) shows a Yb 3d-4f x-ray absorption spectrum (XAS) of $YbRh_2Si_2$. In Fig. 4(b), PES spectra of $YbRh_2Si_2$ in the Yb 3d-4f resonant energy region are displayed. Each of the PES spectra is observed at photon energies as indicated
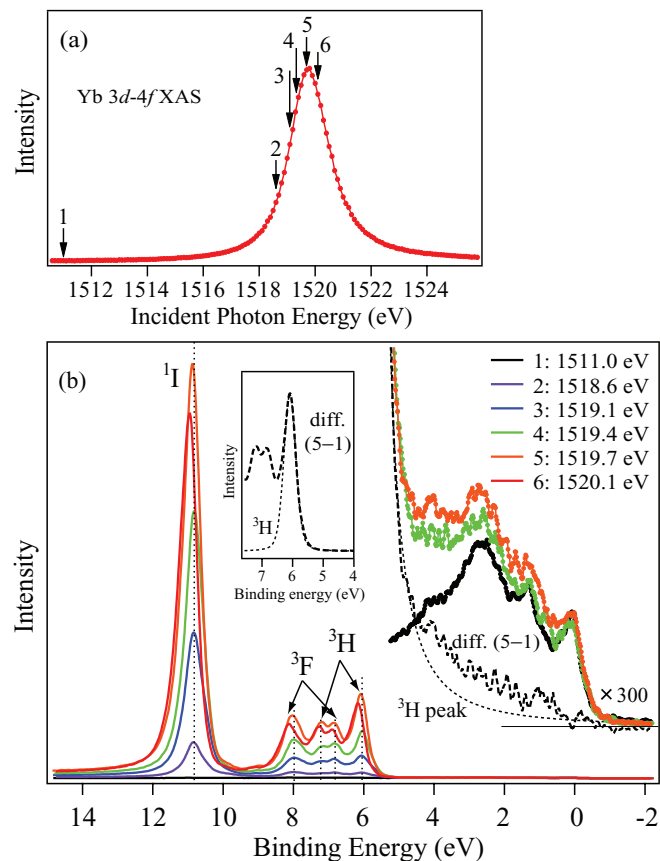
FIG. 4. (Color online) (a) Yb 3d-4f x-ray absorption spectrum and (b) series of AIPES spectra obtained at photon energies indicated in (a). Indices of the multiplet peaks represent the main components of the multiplet states.

in Fig. 4(a). The XAS spectrum has a simple single-peak structure corresponding to the excitation of Yb $3d_{5/2}$ electrons to the Yb^{2+} $4f_{7/2}$ state (the M_5 edge). The shape of the off-resonance spectrum obtained at $h\nu = 1511.0$ eV [1 in Fig. 4(b)] is quite different from the AIPES spectrum obtained at $h\nu = 860$ eV [Fig. 1(a)] due to the difference of the ratio of the atomic cross sections (I) between Yb 4f and Rh 4d states: $I_{Yb4f} : I_{Rh4d} \sim 1 : 1/6$ at $h\nu = 1520$ eV.[15] As we increase the incident photon energy toward the absorption peak, the spectrum shape changes from the off-resonance spectrum. This behavior is quite different from the results of the resonant PES measurement obtained by Yamaoka $et\ al.$, in which the change of the spectrum shape has been observed only at the absorption peak.[19] The branching ratio of the Yb^{3+} is modified in the resonant energy region [2–5 in Fig. 4(b)]. The peaks at $E_B = 6.0$, 7.2, and 10.8 eV are enhanced prominently near the absorption peak. The most enhanced peak at $E_B = 10.8$ eV consists mainly of the ^1I state, and the peaks at $E_B = 6.0$ and 7.2 eV consist mainly of the ^3H state.[17] The resonant enhancement of the Yb^{3+} multiplet has been investigated by using the Yb 4d-4f resonant PES experiment and the theoretical calculation by Schmidt-May $et\ al.$[20] According to their theory, the resonant enhancement of ^1I and ^3H is larger than that of the other states, corresponding to our results. In previous resonant PES studies for Yb-based compounds, multiplet peaks are mixed up and each peak cannot be identified.[19,20] On the other hand, each of the multiplet peaks is clearly distinguished in our Yb 3d-4f resonant PES measurement. Above the absorption peak, the Yb^{3+} peaks shift to the higher binding energies in proportion to the incident photon energy due to the normal Auger process.

Here, we focus on the structure near the Fermi level. The resonant enhancement near E_F is much smaller than that of the Yb^{3+} multiplet. However, one can find the resonant enhancement in this energy region as approaching the incident energy to the absorption peak. The difference spectrum [diff. in Fig. 4(b)] is obtained by subtracting the off-resonance spectrum [1 in Fig. 4(b)] from the on-resonance one [5 in Fig. 4(b)]. We determine the tail of the ^3H peak which is located at the lowest binding energy in the Yb^{3+} multiplet peaks as a convolution of a Lorentzian with a Gaussian, as shown in the inset of Fig. 4(b). The difference spectrum clearly shows a shoulder structure at $E_B = 0$–5 eV, as compared with

the tail of the ^3H peak. This is experimental evidence of the existence of Yb $5d$ electrons in the valence bands. Thus, it is strongly suggested that the charge transfer from the Yb $4f$ to the Yb $5d$ states has an important role in the formation of the valence-band structure of YbRh$_2$Si$_2$.

IV. CONCLUSION

We have presented the 3D valence-band dispersions in the bulk state of YbRh$_2$Si$_2$ using the SX-ARPES measurement. At $T = 15$ K below the T_K, a small Yb^{2+} doublet and a large Yb^{3+} multiplet are observed. This is consistent with previous results indicating that YbRh$_2$Si$_2$ is a valence fluctuation compound. Except the vicinity of Yb $4f$ bands, the experimental valence-band dispersions agree better with those of the LDA calculation

of LuRh$_2$Si$_2$ than those of YbRh$_2$Si$_2$. In line with this, the Yb $3d$-$4f$ resonant PES measurements indicate that the Yb $5d$ electrons exist in the valence band of YbRh$_2$Si$_2$. We suggest that the charge transfer from the Yb $4f$ to the Yb $5d$ orbital is important for the description of the electronic structures of YbRh$_2$Si$_2$ as well as Yb-based heavy fermion compounds.

ACKNOWLEDGMENTS

*a-yasui@spring8.or.jp

[1] P. Gegenwart, J. Custers, C. Geibel, K. Neumaier, T. Tayama, K. Tenya, O. Trovarelli, and F. Steglich, Phys. Rev. Lett. **89**, 056402 (2002).

[2] O. Trovarelli, C. Geibel, S. Mederle, C. Langhammer, F. M. Grosche, P. Gegenwart, M. Lang, G. Sparn, and F. Steglich, Phys. Rev. Lett. **85**, 626 (2000).

[3] J. Custers, P. Gegenwart, H. Wilhelm, K. Neumaier, Y. Tokiwa, O. Trovarelli, C. Geibel, F. Steglich, C. Pepin, and P. Coleman, Nature (London) **424**, 524 (2003).

[4] S. Paschen, T. Luhmann, S. Wirth, P. Gegenwart, O. Trovarelli, C. Geibel, F. Steglich, P. Coleman, and Q. Si, Nature (London) **432**, 881 (2004).

[5] P. Coleman, C. Pepin, Q. Si, and R. Ramazashvili, J. Phys.: Condens. Matter **13**, R723 (2001); Q. Si, S. Rabello, K. Ingersent, and J. L. Smith, Nature (London) **413**, 804 (2001).

[6] A. Hackl and M. Vojta, Phys. Rev. Lett. **106**, 137002 (2011).

[7] S. Watanabe and K. Miyake, Phys. Rev. Lett. **105**, 186403 (2010).

[8] A. B. Sutton, P. M. C. Rourke, V. Taufour, A. McCollam, G. Lapertot, G. Knebel, J. Flouquet, and S. R. Julian, Phys. Status Solidi B **247**, 549 (2010).

[9] A. Yasui, S.-i. Fujimori, I. Kawasaki, T. Okane, Y. Takeda, Y. Saitoh, H. Yamagami, A. Sekiyama, R. Settai, T. D. Matsuda, Y. Haga, and Y. Ōnuki, Phys. Rev. B **84**, 195121 (2011); J. Phys.: Conf. Ser. **273**, 012067 (2011).

[10] See, for example, S. Danzenbächer, Yu. Kucherenko, D. V. Vyalikh, M. Holder, C. Laubschat, A. N. Yaresko, C. Krellner, Z. Hossain, C. Geibel, X. J. Zhou, W. L. Yang, N. Mannella, Z. Hussain, Z.-X. Shen, M. Shi, L. Patthey, and S. L. Molodtsov, Phys. Rev. B **75**, 045109 (2007); G. A. Wigger, F. Baumberger, Z.-X. Shen, Z. P. Yin, W. E. Pickett, S. Maquilon, and Z. Fisk, *ibid.* **76**, 035106 (2007).

[11] D. V. Vyalikh, S. Danzenbacher, Yu. Kucherenko, K. Kummer, C. Krellner, C. Geibel, M. G. Holder, T. K. Kim, C. Laubschat, M. Shi, L. Patthey, R. Follath, and S. L. Molodtsov, Phys. Rev. Lett. **105**, 237601 (2010).

[12] S.-K. Mo, W. S. Lee, F. Schmitt, Y. L. Chen, D. H. Lu, C. Capan, D. J. Kim, Z. Fisk, C.-Q. Zhang, Z. Hussain, and Z.-X. Shen, Phys. Rev. B **85**, 241103(R) (2012).

[13] H. Yamagami, J. Phys. Soc. Jpn. **67**, 3176 (1998).

[14] G. A. Dionicio, Ph.D. thesis, Dresden University of Technology, 2006.

[15] J. J. Yeh and I. Lindau, At. Data Nucl. Data Tables **32**, 1 (1985).

[16] K. Kummer, Yu. Kucherenko, S. Danzenbächer, C. Krellner, C. Geibel, M. G. Holder, L. V. Bekenov, T. Muro, Y. Kato, T. Kinoshita, S. Huotari, L. Simonelli, S. L. Molodtsov, C. Laubschat, and D. V. Vyalikh, Phys. Rev. B **84**, 245114 (2011).

[17] F. Gerken, J. Phys. F **13**, 703 (1983).

[18] B. Kessler, A. Bringer, S. Cramm, C. Schlebusch, W. Eberhardt, S. Suzuki, Y. Achiba, F. Esch, M. Barnaba, and D. Cocco, Phys. Rev. Lett. **79**, 2289 (1997).

[19] H. Yamaoka, I. Jarrige, N. Tsujii, M. Imai, J.-F. Lin, M. Matsunami, R. Eguchi, M. Arita, K. Shimada, H. Namatame, M. Taniguchi, M. Taguchi, Y. Senba, N. Ohashi, N. Hiraoka, H. Ishii, and K.-D. Tsuei, Phys. Rev. B **83**, 104525 (2011).

[20] J. Schmidt-May, F. Gerken, R. Nyholm, and L. C. Davis, Phys. Rev. B **30**, 5560 (1984).